



## THREE-DIMENSIONAL FINITE ELEMENT ANALYSIS OF ADHESIVELY BONDED SINGLE LAP JOINTS IN LAMINATED FRP COMPOSITES SUBJECTED TO COMBINED TRANSVERSE AND THERMAL LOADING (S-S)

\*M. Venkateswara Rao<sup>1</sup>, K. Mohana Rao<sup>2</sup>, V. Rama Chandra Raju<sup>3</sup>,  
V. Bala Krishna Murthy<sup>4</sup> and V.V. Sridhara Raju<sup>4</sup>.

<sup>1</sup>Department of Mechanical Engineering, Bapatla Engineering College, Bapatla, A.P, India.

<sup>2</sup>Department of Mechanical Engineering., K.L. College of Engineering, Vaddeswaram, A.P., India.

<sup>3</sup> J.N.T. U. College of Engineering, Vizayanagaram, A.P., India.

<sup>4</sup>Department of Mechanical Engineering, P. V. P. Siddhartha Institute of Technology, Vijayawada, A.P, India.

### ABSTRACT

The present investigation deals with the thermo-elastic analysis of adhesively bonded single lap joint in laminated FRP composites using three-dimensional theory of elasticity based finite element method. The finite element model is validated with the available results in the literature for the longitudinal loading of a single lap joint (SLJ) made of specially orthotropic laminates and is extended for the analysis of a single lap joint made of generally orthotropic laminates subjected to combined transverse and non-linear temperature loads. The out-of-plane normal and shear stresses are computed at the interfaces of the adherends and adhesive, and at mid surface of the adhesive. The results of the present analysis reveals that the three-dimensional stress analysis is required for the analysis of single lap joint in laminated FRP composites.

**Key words** : SLJ, FEM, FRP, Inter-laminar stresses

### 1.Introduction

Fiber reinforced plastic (FRP) materials have proven to be very successful in structural applications. They are widely used in the aerospace, automotive and marine industries. FRP materials or composites behave differently than typical metals such as steel or aluminum. A typical composite contains layers of aligned fibers oriented at different angles held together by a resin matrix, giving high strength and stiffness in different directions. This anisotropy can cause difficulties when joining two parts together, especially if the two pieces have different stiffness and strength characteristics. The joint can potentially become the weakest link in the structure due to the large amount of load it must transfer. There are wide varieties of ways to join different parts together. Two major methods include mechanical fastening and adhesive bonding. Adhesive bonding of structures has significant advantages over conventional fastening systems. Bonded joints are considerably more fatigue resistant than mechanically fastened structures because of the absence of stress concentrations that occur at fasteners. Joints may be lighter due to the absence of fastener hardware. A major advantage of adhesive bonds is that adhesive bonds may be designed and made in such a way that they can be stronger than the ultimate strength of many metals in common use for aircraft structure. The stresses induced at the interfaces of the

adherends and adhesive play an important role in the design of adhesively bonded joints in FRP composites. Hence, these stresses are required to be analyzed most accurately.

In 1938, Volkersen [1] first proposed a simple shear lag model for mechanical joints with many fasteners, and later on, this model was adopted for adhesively bonded lap joints with the assumption that the adherends are in tension and adhesive is in shear only and both stresses are constant across the thickness. In 1944, Goland and Reissner [2] took into consideration the effects of the adherends bending and the peel stress, as well as the shear stress, in the adhesive layer in a single lap joint. Subsequent efforts by Oplinger [3] suggested corrections to the Goland and Reissner solution by using a layered beam theory instead of classical homogeneous beam model for single lap joints. The corrections in the shear lag model, or Volkersen solution, include works by Hart-Smith [4,5] and Tsai et.al [6]. Hart-Smith [4,5] modified the shear lag model to include the effect of adhesive plasticity. Tsai et.al [6] provided a correction to the shear lag model with the assumption that the shear stress is linear through the adherends. The analysis of Klarbring and Movchan [7] involved mathematically modeling the adhesive joint using an asymptotic approach. Kim and Kedward [8] used finite difference method for the analysis of adhesively bonded joints. Penado and Dropek [9] and Tessler et.al [10] used finite element method for the analysis of adhesively bonded joints.

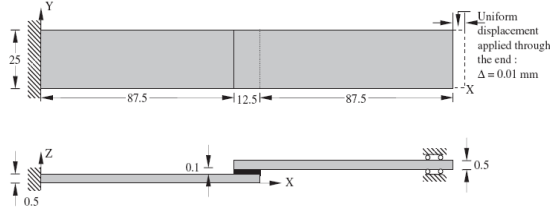
Adams and Peppiatte [11] analyzed a bonded joint using a two dimensional linear elastic finite element method with plane strain assumption. Examples of finite element investigations of adhesively bonded composite joints include Kairouz and Matthews [12], Tong [13], Li et al. [14]. Delale et al. [15] developed a closed-form solution for lap-shear joints with orthotropic adherends using classical plate theory. Mortensen [16] presented a unified analytical approach to analyze an array of common bonded joint configurations for more general loading conditions. Panigrahi and Pradhan [17] studied a single lap joint with the adherends made of specially orthotropic laminates for the evaluation of the tri-axial stress field using finite element analysis and proved the necessity of three-dimensional stress analysis of single lap joint. Venkateswara Rao et al analyzed a single lap joint in FRP composites subjected to axial and transverse pressure loads with adherends made of generally orthotropic laminates [18,19].

The objective of the present paper is to extend the three-dimensional stress analysis of Venkateswara Rao et al [18] for the single lap joint subjected to non-linear temperature distribution and transverse loads (SS). The analysis includes the evaluation of i) Inter-laminar normal stress ( $\sigma_{zz}$ ), ii) Inter-laminar shear stress in longitudinal plane ( $\tau_{zx}$ ) and iii) Inter-laminar shear stress in transverse plane ( $\tau_{yz}$ ) at the interfaces of the adherends and adhesive, and at the middle plane of the adhesive.

## 2. Problem Modeling

### 2.1 Geometry

The geometry of the lap joint for longitudinal loading (used for the validation purpose) is as shown in Fig. 1. In case of transverse loading, the thickness of the adherends is increased to maintain the length-to-thickness ratio (s) equal to 10. The thickness of the adhesive is increased proportionately with the thickness of the adherends. The in-plane dimensions for the transverse loading are same as that of longitudinal loading.



All dimensions are in mm

**Fig. 1 Geometry of the single lap joint**

### 2.2 Finite Element Model

The finite element mesh is generated using a

three-dimensional brick element ‘SOLID 45’ of ANSYS [20]. This element (Fig. 2) is a structural solid element designed based on three-dimensional elasticity theory and is used to model thick orthotropic solids. The element is defined by 8 nodes having three degrees of freedom per node: translations in the nodal x, y, and z directions.

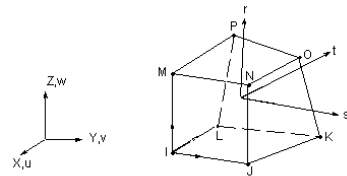


**Fig. 2 SOLID 45 Element**

### 2.3 Loading

The following types of loads are applied for validation and prediction of the response of the structure for the present analysis.

- i) A uniform longitudinal displacement of 0.01 mm for the validation purpose.

A combined load consisting of a uniform transverse load of 1 MPa and non-linear temperature load obtained from thermal analysis with following conditions is applied:

- a. 100°C on top surface of the joint
- b. Convection at bottom, side faces and both the ends of the joint with  $h = 5 \text{ W/m}^2\text{K}$  and  $T_\infty = 30^\circ$ .

### 2.4 Boundary Conditions

Both the ends of the joint are simply supported

### 2.5 Material Properties [21]

The following mechanical properties are taken for the thermoelastic analysis of single lap joint.

#### i) Epoxy (adhesive)

$E = 5.171 \text{ GPa}$ ;  $\nu = 0.35$ ;  
 $k = 0.18 \text{ W/m K}$ ;  $\alpha = 72 \times 10^{-6} / ^\circ\text{C}$

#### ii) Graphite-Epoxy (adherends)

$K_L = 36.42 \text{ W/m K}$                        $K_T = 0.96 \text{ W/m K}$   
 $E_1 = 172.72 \text{ GPa}$ ,                       $E_2 = E_3 = 6.909 \text{ GPa}$   
 $G_{12} = G_{13} = 3.45 \text{ GPa}$ ,               $G_{23} = 1.38 \text{ GPa}$ ,  
 $\nu_{12} = \nu_{13} = \nu_{23} = 0.25$   
 $\alpha_1 = 0.57 \times 10^{-6} / ^\circ\text{C}$                $\alpha_2 = \alpha_3 = 35.6 \times 10^{-6} / ^\circ\text{C}$

### 2.6 Laminate sequence

i) Two  $0^\circ/90^\circ/90^\circ/0^\circ$  laminated FRP composite plates are used as adherends for the validation of present FE model with reference [17].

ii) Two  $+\theta^\circ/-\theta^\circ/-\theta^\circ/+\theta^\circ$  laminated FRP composite plates are used as adherends for the present analysis. The

value of  $\theta$  is measured from the longitudinal direction of the structure (x-axis) and varied from  $0^\circ$  to  $90^\circ$  in steps of  $15^\circ$ .

### 3. Results

#### 3.1 Validation

Fig. 3 shows the finite element mesh on the overlap region of the single lap joint. The present finite element model is validated by comparing the stresses obtained for the single lap joint of specially orthotropic laminates with the results of reference [17] for longitudinal loading. Table. 1 shows the comparison of maximum values of the stresses at the specified locations and close agreement is found. Later this model is extended for the analysis of single lap joint of generally orthotropic laminates subjected to combined transverse and non-linear temperature loading.

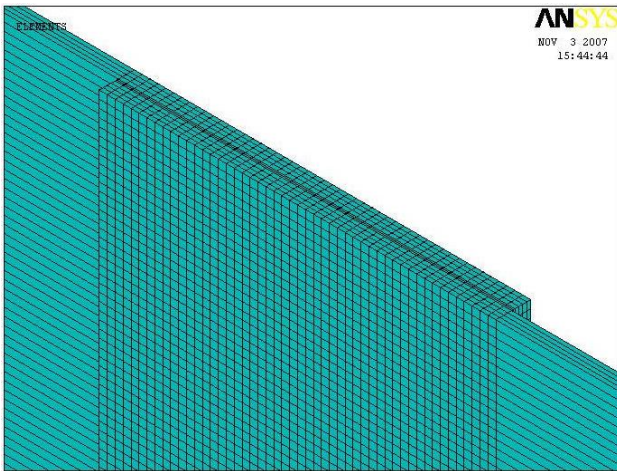


**Fig. 3 Finite element mesh on the overlap region of the single lap joint**

**Table 1. Validation of the finite element model**

Location	$\sigma_{zz}$ (MPa)		$\tau_{yz}$ (MPa)		$\tau_{zx}$ (MPa)	
	Ref [17]	Present	Ref [17]	Present	Ref [17]	Present
Top Interface	0.40	0.41	0.08	0.14	0.39	0.40
Bottom Interface	0.39	0.39	0.08	0.13	0.38	0.39

#### 3.2 Variation of the stresses across the width of the laminate

One of the reasons for the variation of the stresses across the width of the laminate is due to the non-uniform arrangement of the fibers in the width direction except at  $\theta = 0^\circ$  and  $90^\circ$ . The second reason is due to the coupling

between bending, shear, and extensions in the deformations of the laminates. Another reason is due to the inter-laminar effect at the free edges of the structure.

Variation of normal stress  $\sigma_{zz}$  across width for several fiber angles is shown in Fig.4. This stress for  $\theta=0^\circ$  increases up to  $y=12.5\text{mm}$  later decreases. For  $\theta=30^\circ$  the stress is continuously increasing with intermediate dips with minimum value at  $y=0\text{mm}$  and maximum value at  $y=25\text{mm}$ . Variation of stress for  $\theta=45^\circ$  and  $60^\circ$  is zig-zag across the width of joint. This stress for  $\theta=90^\circ$  is flat between  $5\text{mm}$  and  $20\text{mm}$  followed by decrease and slight increase of stress at both the ends of joint.

Fig.5 depicts the variation of  $\tau_{yz}$  for several fiber angles across the width. For  $\theta=0^\circ$  and  $90^\circ$ , this stress is maximum at the ends and zero at the middle of joint i.e at  $y=12.5\text{mm}$ . For  $\theta=30^\circ, 45^\circ$  and  $60^\circ$ , this stress increases between  $0\text{mm}$  and  $5\text{mm}$ , later decreases with minimum stress at  $y=25\text{mm}$ .

Fig. 6 illustrates the variation of shear stress across the width of joint for several fiber angles. For  $\theta=0^\circ, 30^\circ, 45^\circ$  and  $60^\circ$ , this stress increases enormously between  $0\text{mm}$  and  $5\text{mm}$ , later the variation of stress between  $5\text{mm}$  and  $20\text{mm}$  is less, followed by decline of stress at the end of the joint. This stress for  $\theta=90^\circ$  is flat between  $5\text{mm}$  and  $20\text{mm}$  followed by decrease of stress and increase of stress at both the ends.

In most of the above cases, it is observed that the stresses are maximum near the ends of the plate in the width direction. This may be due to the inter-laminar effect in addition to the coupling effect. The stresses shown in Figs. 4-6 are measured at the locations where the normal and shear stresses are maximum in the bottom interface of the adherend and adhesive.

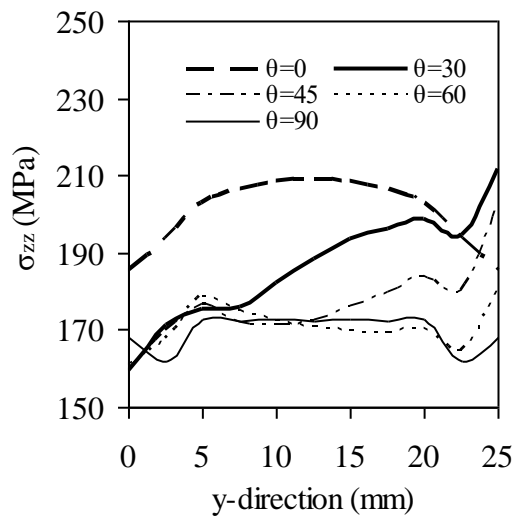


**Fig. 4. Variation of  $\sigma_{zz}$  across width**

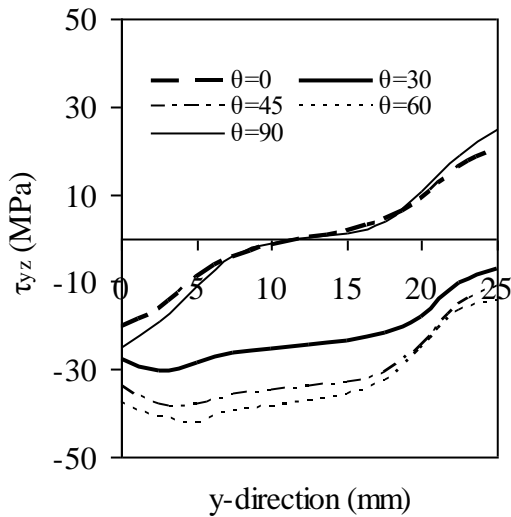


Fig. 5. Variation of  $\tau_{yz}$  across width

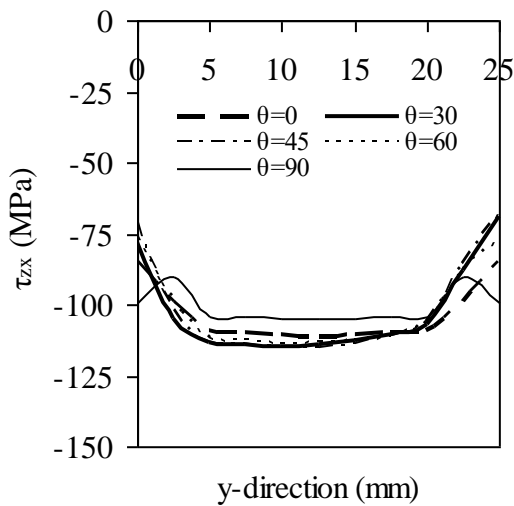


Fig. 6. Variation of  $\tau_{zx}$  across width

### 3.3 Variation of the maximum stresses with respect to the fiber angle $\theta$

Load transfer between adjacent layers in a fiber-reinforced laminate takes place by means of interlaminar stresses, such as  $\sigma_{zz}$ ,  $\tau_{zx}$ , and  $\tau_{yz}$ . The principal reason for the existence of interlaminar stresses is the mismatch of Poisson's ratios  $\nu_{xy}$  and coefficients of mutual influence and between adjacent laminas. If the laminas were not bonded and could deform freely, an axial loading in x-direction would create dissimilar transverse strains  $\epsilon_{yy}$  in various laminas because of the difference in their Poisson's ratios. However, in perfect bonding, transverse strains must be identical throughout the laminate. The constraint against free transverse

deformations produces normal stress  $\sigma_{yy}$  in each lamina and interlaminar shear stress  $\tau_{yz}$  at the lamina interfaces. Similarly, the difference in the coefficients of mutual influence would create dissimilar shear strains  $\gamma_{xy}$  in various laminas only if they were not bonded. For a bonded laminate, equal shear strains for all laminas require the development of interlaminar shear stress  $\tau_{zx}$ . Although the force equilibrium in the y-direction is maintained by the action of  $\sigma_{yy}$  and  $\tau_{yz}$ , the force resultants associated with  $\sigma_{yy}$  and  $\tau_{yz}$  are not collinear. The moment equilibrium about the x-axis is satisfied by the action of the interlaminar normal stress  $\sigma_{zz}$ . [22]. In addition the mismatch of coefficients of thermal expansion will also cause for the inter-laminar stresses in thermal loading. In general case of loading the interlaminar stresses will be developed due to all of the above reasons. As the fiber angle  $\theta$  increases the mismatch in the Poisson's ratios of adherend and adhesive decreases up to certain angle and later increases, and the same trend can be expected in the variation of interlaminar stresses with respect to fiber angle. The effect of coefficients of mutual influence is to raise the stresses up to certain value of  $\theta$  and later the stresses decrease.

As the fiber angle  $\theta$  varies from  $0^\circ$  to  $90^\circ$ , the mismatch between the coefficients of thermal expansion of adherend and adhesive increases resulting in increase in stresses with respect to  $\theta$ .

As the force transmission takes place through the interlaminar stresses from the adherend to adhesive, the stresses at the mid plane of adhesive will also be affected by the fiber angle.

Fig. 7 shows the variation of normal stress  $\sigma_{zz}$  on various surfaces with fiber angle  $\theta$ . This stress on bottom interface decreases between  $0^\circ$  and  $15^\circ$  due to reduction of mismatch in Poisson's ratio of adhesive and adherend, increases between  $15^\circ$  and  $30^\circ$  due to resultant influence of effect of mutual influence and coefficient of thermal expansion. Beyond  $30^\circ$  this stress declines due to mutual influence. This stress on top interface increases up to  $\theta=60^\circ$  due to effect of mutual influence and mismatch in coefficient of thermal expansion of adhesive and adherend later slight decrease of stress due to effect of mutual influence. Slight decrease of stress between  $0^\circ$  and  $15^\circ$ , later slight increase of stress between  $15^\circ$  and  $30^\circ$  followed by slight drop in stress is noticed on mid surface.

Fig. 8 depicts the variation of shear stress  $\tau_{yz}$  with fiber angle  $\theta$  on various surfaces. This stress on mid surface, top interface and bottom interface increases up to  $45^\circ$ ,  $60^\circ$  and  $60^\circ$  respectively due to resultant influence of effect of mutual influence and mismatch in coefficient of thermal expansion of adhesive and adherend later decreases due to effect of mutual influence.

Fig. 9 illustrates the variation of shear stress  $\tau_{zx}$

with  $\theta$  on various surfaces. This stress increases slightly between  $0^\circ$  and  $90^\circ$  on mid surface due to mutual influence and  $\alpha$  up to  $45^\circ$ , later due to  $\alpha$  and  $v$ , where as on top interface this stress decreases slightly due to  $v$  up to  $45^\circ$ , later due to mutual influence. Slight increase of stress up to  $45^\circ$  and slight decrease of stress beyond  $45^\circ$  is noticed on bottom interface. However this stress shows the largest response on bottom interface at all the fiber angles.

The variation of transverse deflection 'w' with fiber angle  $\theta$  is shown in Fig.10. The deflection, minimum at  $\theta = 0^\circ$  and maximum at  $\theta = 90^\circ$ , increases gradually with fiber angle  $\theta$ . The factors influencing the deflection are variation of stiffness and mutual influence with  $\theta$ .

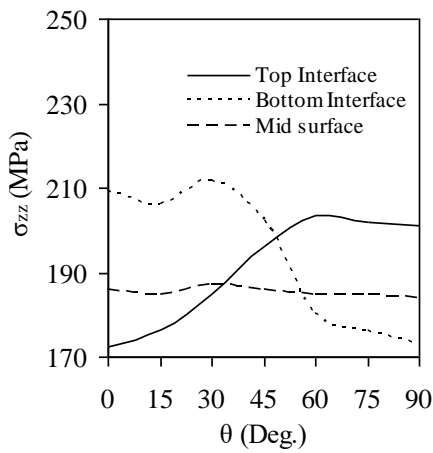


Fig. 7. Variation of  $\sigma_{zz}$  with  $\theta$

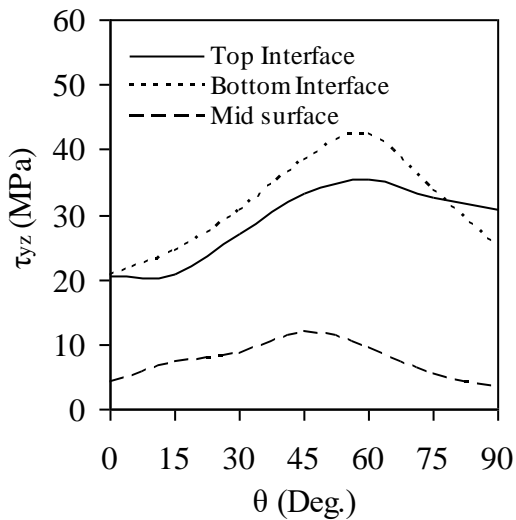


Fig. 8. Variation of  $\tau_{yz}$  with  $\theta$

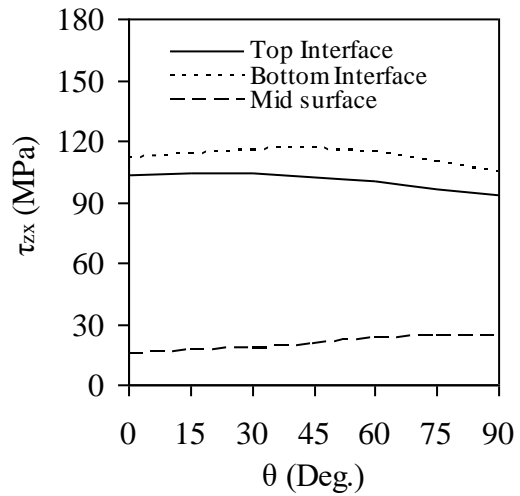


Fig. 9. Variation of  $\tau_{zx}$  with  $\theta$

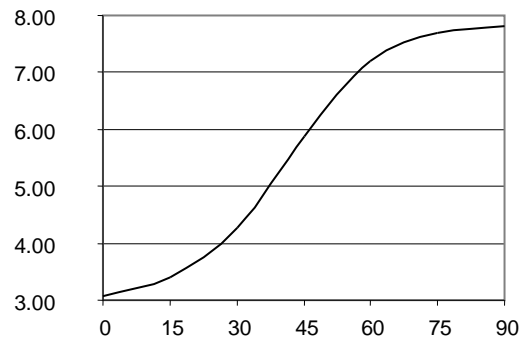


Fig. 10. Variation of 'w' with  $\theta$

#### 4. Conclusions

Three-dimensional finite element analysis has been taken up for the evaluation of the inter-laminar stresses at the interfaces of the adherends and adhesive, and the out-of-plane stresses at the middle surface of single lap joint made of FRP laminates of generally orthotropic nature subjected to combined transverse and non-linear temperature loads(SS). The following conclusions are drawn:

- Variation of the stresses in the width direction is significant and therefore three-dimensional analysis is necessary.
- The intensity of normal stress is found to be maximum on bottom interface at lower fiber angles. As the normal stress intensity is less at higher fiber angles,  $60^\circ$  to  $90^\circ$  fiber angle range is suitable in order to avoid the interfacial failure at the bottom interface.

- It is also observed that the coupling effect in the laminate influences the deflection and stresses, and causing for the increase in their magnitudes up to some value of fiber angle and then decreasing of the values later.

## 5. References

1. Volkersen, O., 1938, "Die Niekraftverteilung in Zugbeanspruchten mit Konstanten Laschenquerschnitten. Luftfahrtforschung", 15, pp. 41–47.
2. Goland, M. and Reissner, E., 1944, "The Stresses in Cemented Joints", ASME Trans., Journal of Applied Mechanics, 11, pp.17–27.
3. Oplinger, D. W., 1991, "A Layered Beam Theory for Single Lap Joints", Army Materials Technology Laboratory Report, MTL TR91–23.
4. Hart-Smith, L. J., 1973, "Adhesive-Bonded Single Lap Joints", NASA-CR-112236.
5. Hart-Smith, L. J., 1973, "Adhesive-bonded Double Lap Joints", NASA-CR-112235.
6. Tsai, M. Y., Oplinger, D. W. and Morton, J., 1998, "Improved Theoretical Solutions for Adhesive Lap Joints", Int. Journal of Solids Structures, 35(13), pp.1163–1185.
7. Klarbring, A. and Movchan A.B., 1988, "Asymptotic modeling of adhesive joints", Mechanics of materials, 28, pp.137-145.
8. Kim H. and Kedward K., 2001, "Stress analysis of adhesively bonded joints under in plane shear loading", J. Adhesion, 76, pp.1-36
9. Penado F.E. and Dropek R.K., 1990, "Numerical design and analysis", Engineered materials Hand book, 3, Adhesives and Sealants, ASM International.
10. Tessler, A., Dambach M.L. and Oplinger D. W., 2000, "Efficient adaptive mesh refinement modeling of adhesive joints", presented at the work shop on bonded joints and assemblies in aircraft, ASTM/ASC, Texas A&M
11. Adams, R. D. and Peppiatt, N. A., 1974, "Stress Analysis of Adhesively Bonded Lap Joints", Journal of Strain Analysis, 9, pp.185–196.
12. Kairouz, K. C. and Matthews, F. L., 1993, "Strength and Failure Modes of Bonded Single Lap Joints between Cross-Ply Adherends", Composites, 24(6), pp.475–484.
13. Tong, L. and Steven, G. P., 1999, "Analysis and Design of Structural Bonded Joints", Kluwer Academic Publishers.
14. Li, Gang and Lee-Sullivan, Pearl, 2001, "Finite Element and Experimental Studies on Single-lap Bonded Joints in Tension", Int. Journal of Adhesion and Adhesives, 21(3), pp. 211–220.
15. Delale, F., Erdogan, F. and Aydinoglu, M. N., 1982, "Stresses in Adhesively Bonded Joints: A Closed-form Solution", Journal of Composite Materials, 15, pp.249–271.
16. Mortensen, F. and Thomsen, O. T., 2002, "Analysis of Adhesive Bonded Joints: A Unified Approach", Composite Science and Technology, 62(7–8), pp.1011–1031.
17. Panigrahi, S. K. and Pradhan, B., 2007, "Three dimensional Failure analysis and damage Propagation behavior of Adhesively bonded Single lap joints in laminated FRP Composites", Journal of Reinforced plastics and Composites, 26(2), pp.183-201.
18. Venkateswara Rao, M., Mohana Rao, K., Rama Chandra Raju, V., Bala Krishna Murthy, V. and Sridhara Raju, V.V., 2007, "Three-Dimensional Finite Element Analysis of Adhesively Bonded Single Lap Joints in Laminated FRP Composites", International Journal of Materials Sciences, 2(3), pp. 309–319.
19. Venkateswara Rao, M., Mohana Rao, K., Rama Chandra Raju, V., Bala Krishna Murthy, V. and Sridhara Raju, V.V., 2007, "Analysis of Adhesively Bonded Single Lap Joints In Laminated FRP Composites subjected to Transverse Load", Accepted for publication in International Journal of Mechanics and Solids.
20. ANSYS reference manuals (2006).
21. Tungikar VB, and Rao KM., 1994, "Three dimensional exact solution of thermal stresses in rectangular composite laminate", Composite Structures, 27, pp.419-430.
22. Mallick, P. K., 1988, "Fiber-Reinforced Composites", MARCEL DEKKER, INC., pp.159-162.